Progress of Theoretical Physics, Vol. 71, No. 5, May 1984

# Scenarios Leading to Chaos in a Forced Lotka-Volterra Model

Masayoshi INOUE and Hiroshi KAMIFUKUMOTO

*Department of Physics, Kagoshima University, Kagoshima 890*

(Received December 6, 1983)

A predator-prey ecosystem is proposed to investigate roads to chaos in a differential system. In this model, Malthusian rate of prey is driven by a periodic external force. Feigenbaum scenarios and a torus to chaos with frequency locking as 1→torus→5→chaos→4→chaos→3→chaos→5→chaos→4→2 are observed numerically and their scaling properties and multi-basins are investigated.

## § 1. Introduction

There are two important models to discuss population dynamics of ecosystems. One of the two is a differential logistic model for a one-species ecosystem. The model can well explain an observed saturation phenomenon of a population of an ecosystem such as a bacterium in a test tube. The other model is the Lotka-Volterra model which was proposed to interpret a periodic oscillation of the two populations in a predator-prey ecosystem.

A discrete version of the logistic model has been used when a generation of a species is non-overlapping.[1] In 1974, May[2] discovered numerically that the logistic difference equation gives a period doubling bifurcation and a chaotic motion. A noisy oscillation of a fly's population, which was observed by Nicholson,[3] is considered as an example of the chaotic motion. Since the pioneering work of May, there are many studies on chaotic behavior of deterministic dynamical systems, but there are only a few studies on the predator-prey ecosystem from the viewpoint of chaos.[4],[5]

In this paper we introduce a modified Lotka-Volterra model and study scenarios leading to chaos, where we will find that Feigenbaum scenario,[5] namely the period doubling scenario, coexists with a torus to chaos scenario. The torus to chaos scenario was observed in the Rayleigh-Bénard system[7] and the phenomenon was studied by using a map of a circle onto itself.[8]~[12] However, only a few studies were carried out in a differential system.[13] The set of differential equations of our model is introduced in §2. The torus to chaos scenario and the scaling property of the frequency locking states are investigated in §3. Feigenbaum scenarios and some multi-basins are found in §4. Section 5 is devoted to discussion and some remarks.

## § 2. Model and its equations of motion

The original Lotka-Volterra model is described by the following pair of equations:[14]

$$\frac{dN_1}{dt}=\alpha_1 N_1-\beta_1 N_1 N_2\,, \tag{1}$$

$$\frac{dN_2}{dt}=-\alpha_2 N_2+\beta_2 N_1 N_2\,, \tag{2}$$

where $\alpha_1$ is the Malthusian rate of prey, $\alpha_2$ is the die out rate of predator, and $N_1$ and $N_2$ are the populations of prey and predator, respectively. The term $-\beta_1 N_1 N_2$ represents the loss rate of prey due to collisions with predator, and $\beta_2 N_1 N_2$ represents the growth rate of the population of predator through the same collisions. This model gives a periodic solution but the periodicity and the amplitude of it depend on its initial condition and the model has lack of a structual stability.[15] A stable limit cycle solution is necessary to explain the observed oscillative populations of prey and predator.[16] Various modified Lotka-Volterra models have been proposed by many authors.[17] Gause[18] obtained a reasonable collision term which proportional to $\sqrt{N_1}$.*) We modify the collision terms in Eqs. (1) and (2) according to Gause's result and obtain

$$\frac{dN_1}{dt} = \alpha_1 N_1 - \beta_1 \sqrt{N_1} N_2 - \gamma_1 N_1^2 , \tag{3}$$

$$\frac{dN_2}{dt} = -\alpha_2 N_2 + \beta_2 \sqrt{N_1} N_2 , \tag{4}$$

where the logistic term $\gamma_1 N_1^2$ is introduced. The original Lotka-Volterra's collision terms are proportional to $N_1$ but in this case they are proportional to $\sqrt{N_1}$ that provide

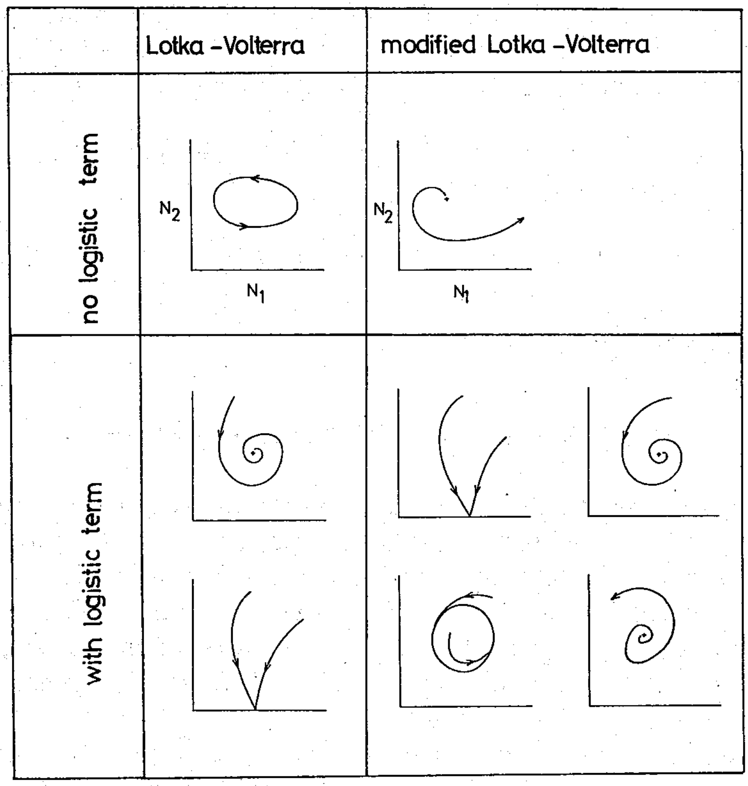


Fig. 1. The possible types of motions in the Lotka-Volterra model (Eqs. (1) and (2)) and the modified Lotka-Volterra model (Eqs. (3) and (4)). A logistic term is added to Eq. (1) in the lower part of the left column.

*) Gause's collision is obtained if only the surface part, whose population is proportional to $\sqrt{N_1}$, of the prey-community contributes to the collision.

a saturation effect for the collision. The saturation effect causes a population explosion of prey when the logistic term is disregarded. If we put the logistic term to the original Lotka-Volterra model, the periodic solution disappears. On the other hand, the term together with Gause's collision terms brings us some limit cycles for certain parameter regions. These results are easily obtined by the method of isoclines and stability theory,[15] and these are summarized in Fig. 1.

The limit cycle solution gives a simple oscillative evolution of the two populations. However, in a real two-species ecosystem such as mountain cat-hare community,[19] the periodic oscillation is not so simple but it seems a weakly chaotic oscillation. We will propose a predator-prey model in which the evolution of the two populations chaotically oscillates without external noise.

It needs more than three variables to get a chaotic solution in a differential system. Therefore, a two-species ecosystem with a time dependent external force or an $n$-species ($n \geqq 3$) ecosystem[5] has a possibility to behave chaotically. In this paper we choose the former one. We assume that the environment of prey changes periodically. Then the Malthusian rate in Eq. (3) turns out to be

$$\alpha_1(t)=2(a-b\cos\omega t), \tag{5}$$

where $a$ is the positive constant and, $b$ and $\omega$ are the amplitude and the angular frequency of the oscillative part of the Malthusian rate, respectively. Time-delay due to recovery of grass causes a periodic oscillation of grass-eating animal's population.[20] The Malthusian rate Eq. (5) is considered to be one of the effective expression of the oscillative phenomenon.

We introduce the variables $x\equiv\sqrt{N_1}$ and $y\equiv N_2$, thus our model (Eqs. (3) and (4) with Eq. (5)) can be expressed as

$$\frac{dx}{dt}=(a-b\cos\omega t)x-(\beta_1/2)y-(\gamma_1/2)x^3, \tag{6}$$

$$\frac{dy}{dt}=-\alpha_2 y+\beta_2 xy. \tag{7}$$

## § 3. Torus to chaos with frequency locking

In this section, we investigate numerically the scenario leading to chaos where we choose a parameter set $a=\alpha_2=3.0$, $(\beta_1/2)=\beta_2=1.5$ and $\gamma_1=0.48$. This parameter set with no external field $b=0$ gives a limit cycle whose angular frequency takes 2.3. The limit cycle is modulated by the external periodic force and various types of the motion appear in the $b$-$\omega$ phase diagram. Interesting scenarios are observed in the range $2.5\leqq\omega\leqq4.0$ with $b=0.17$ and a coarse diagram is shown in Fig. 2 where Runge-Kutta-Gill method has been used to solve the set of Eqs. (6) and (7).

In the lower frequency part of the region, the limit cycle with $b=0$ is entrained by the periodic external force because its frequency is nearly equal to the frequency of the external force. As $\omega$ is increased from the lower frequency, a Hopf bifurcation takes place at $\omega=2.64$ then the entrained limit cycle becomes a torus. A new fundamental frequency, which is incommensurate with $\omega$, appears with the aid of the bifurcation. After the quasi-periodic motion has come to an end, a significant phenomenon of frequency

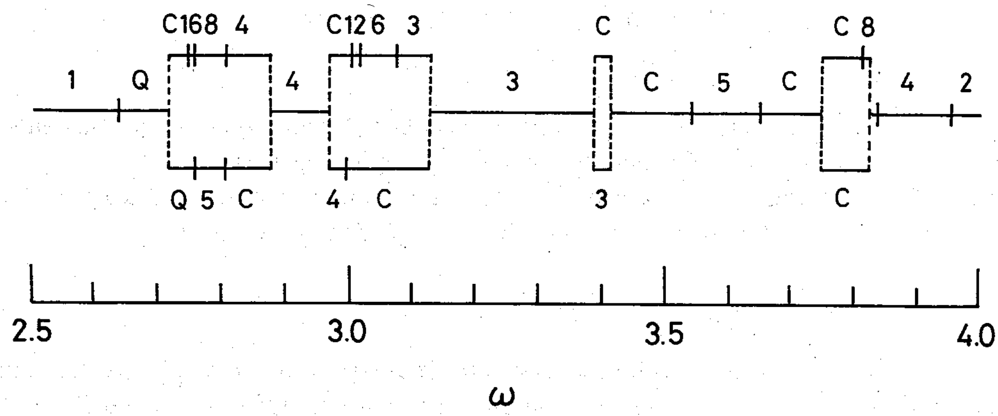


Fig. 2. The coarse phase diagram of Eqs. (6) and (7) where parameters are taken as $a=\alpha_2=3.0$, $(\beta_1/2)=\beta_2=1.5$, $\gamma_1=0.48$ and $b=0.17$. The quasi-periodic and chaos are represented as $Q$ and $C$, respectively. The $n$-cycle is denoted by $n$.

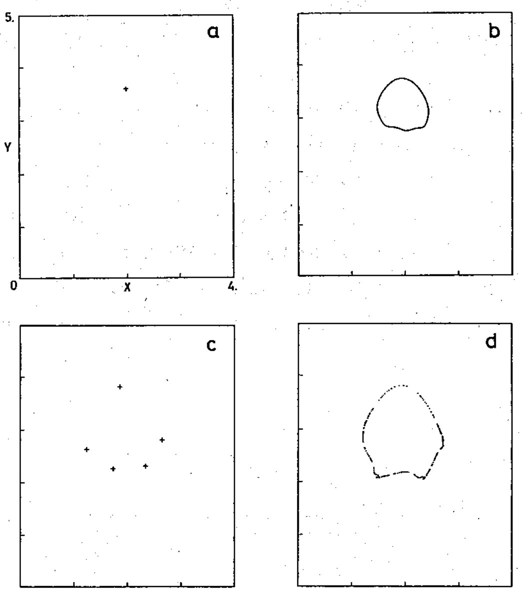


Fig. 3. Poincaré mappings of the torus to chaos with frequency locking scenario where parameters are taken as $a=\alpha_2=3.0$, $(\beta_1/2)=\beta_2=1.5$, $\gamma_1=0.48$ and $b=0.17$. The angular frequencies are chosen as (a) $\omega=2.65$, (b) $\omega=2.70$, (c) $\omega=2.76$ and (d) $\omega=2.87$.

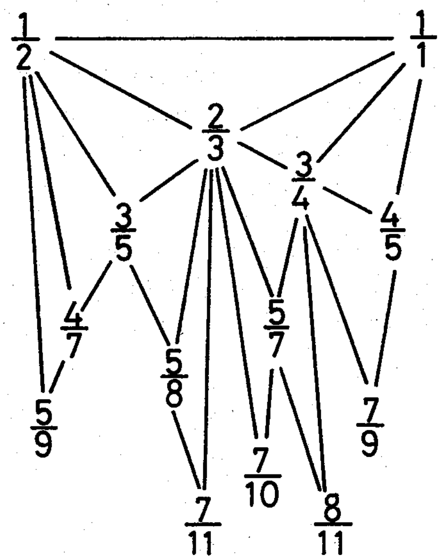


Fig. 4. Topology of Farey series of order 11 where observed winding numbers are used.

locking occurs at $\omega=2.76$. In this scenario, chaos sets in at $\omega=2.81$. The scenario is summarized as: *entrained limit cycle → torus → frequency locking → chaos.* This may be regarded as a typical one leading to chaos in a periodically forced system with dissipation. The scenario is illustrated in Fig. 3 by Poincaré mappings in which successive points specifying the state of the system are plotted in the $x$-$y$ plane at instants separated by a regular time interval $T=2\pi/\omega$.

In a wide range, a period-decreasing sequence is found

$$1 \to \text{torus} \to 5 \to \text{chaos} \to 4 \to \text{chaos} \to 3$$

$$\to \text{chaos} \to 5 \to \text{chaos} \to 4 \to 2\,,$$

as we increase $\omega$ from 2.5 to 4.0. Period-adding sequence was found in various fields, and it was studied with the use of a one-dimensional mapping by Kaneko.[10),11)]

In a fine phase diagram, there are many frequency locking states and to relate all the different periods, we introduce a winding number $\rho$ which is calculated as

$$\rho = \lim_{n\to\infty} \sum_{i=1}^{n} \frac{\theta_i - \theta_{i-1}}{n}\,, \tag{8}$$

where $\theta_i$ is the angle of the $i$th point measured from an appropriate origin given inside the invariant closed curve in the Poincaré mapping. When the state is characterized by the two fundamental frequencies, the winding number $\rho$ is the ratio between the two. The winding number is a monotonically decreasing function of $\omega$. If there are two locking states, whose winding numbers are $\rho_1 = q_1/p_1$ and $\rho_2 = q_2/p_2$, a locking state of $\rho_3 = (q_1+q_2)/(p_1+p_2)$ exists between the two locking states in the region $\omega$. We diagram a tree, which leads to a Farey series, using observed winding number. The tree is shown in Fig. 4.

The frequency dependence of the winding number is shown in Fig. 5 where every frequency locking state gives a step for each rational value of the winding number. The steps compose a staircase and such a curve with infinitely many steps is called a devil's staircase. The step's width $(\omega_n - \omega_{n-1})$, where $\omega_n$ is the set on frequency of the locking state whose winding number is $\rho_n$, depends on $\rho_n$ and it is wide for a low order $\rho_n$ such as 4/5, 3/4, 2/3 and 3/5. We study scaling property of frequency locking sequence where we treat the series $\rho_n = 3n/(4n-1)$, which accumurate to $\rho_\infty = 3/4 (n \to \infty)$. The result is shown in Fig. 6 which shows

$$(\omega_n - \omega_\infty) \propto n^{-2.0}\,. \tag{9}$$

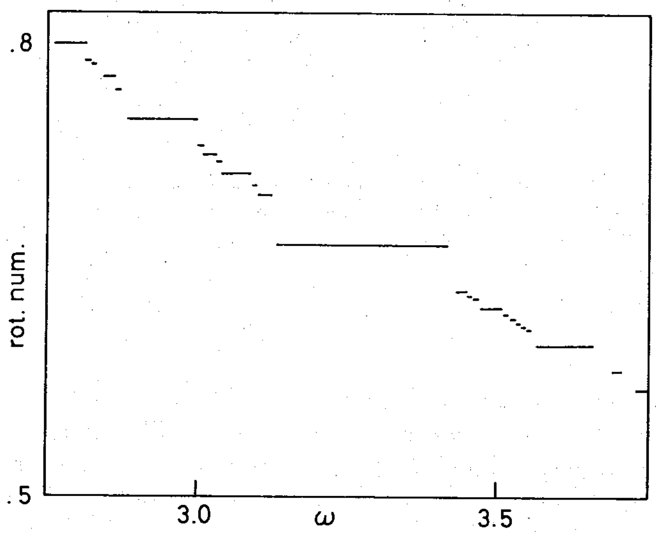


Fig. 5. Graph of winding number $\rho$ against the angular frequency $\omega$ in correspondence of the periodic states found in the interval (2.75, 3.75).

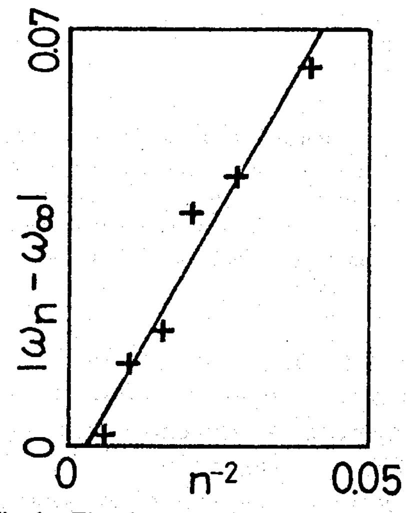


Fig. 6. The observed scaling law for the series $\rho_n = 3n/(4n-1)$.

This result agrees with Kaneko's[10] result on a map and Sano and Sawada's[13] result on a coupled nonlinear oscillator.

## § 4. Feigenbaum scenarios and multiple steady states

In this section we decrease the angular frequency $\omega$ from 4.0 to 2.5 and other parameters are taken as the same as the preceding section. We take the reverse of the preceding section's course. In this course we observed a Feigenbaum scenario of $2\times 2^n$, in which a cascade of period doubling leads to a chaos. The Poincaré mappings of this scenario are shown in Fig. 7.

In the chaotic case, Fig. 7(c), the mapping is represented by the asymptotic invariant manifold which consists of four islands. The phase point transits regularly the four islands but in each island the motion of the phase point is chaotic. The invariant manifold is a strange attractor which is created by the processes of an enlargement, a folding and a pressing which are similar to the processes of the baker's transformation in Bernoulli system. These processes can be easily visualized with the aid of a time development of $x$ which is shown in Fig. 8.

The above two islands in Fig. 7(c) are merged as the angular frequency $\omega$ is decreased. The merged island is shown in Fig. 7(d), and the phase point moves chaotically on the merged island. A symmetry change of the chaos due to the merging has been already discussed by Fujisaka and the authors.[21] Feigenbaum scenarios of $3\times 2^n$ and $4\times 2^n$ are found also as already shown in Fig. 2. We calculate a ratio $\delta=(\omega_3-\omega_6)/(\omega_6-\omega_{12})$ for the $3\times 2^n$-cascade and obtain $\delta=4.754$ which is nearly equal to Feigenbaum

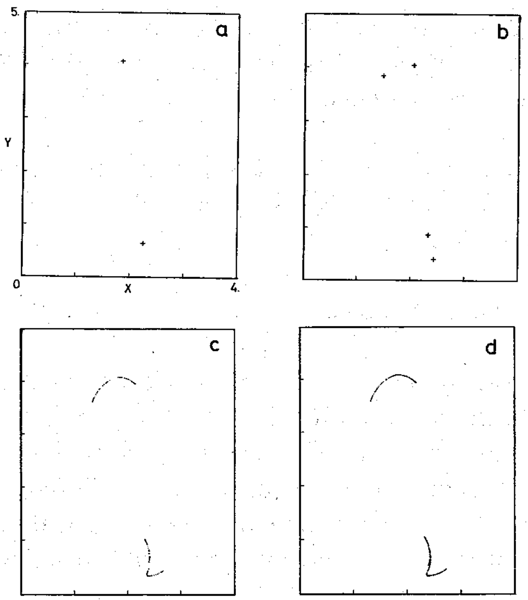


Fig. 7. Poincaré mappings of the Feigenbaum scenario of $2\times 2^n$ where parameters are taken as $a=\alpha_2=3.0$, $(\beta_1/2)=\beta_2=1.5$, $\gamma_1=0.48$ and $b=0.17$. The angular frequencies are chosen as (a) $\omega=3.96$, (b) $\omega=3.84$, (c) $\omega=3.79$ and (d) $\omega=3.78$.

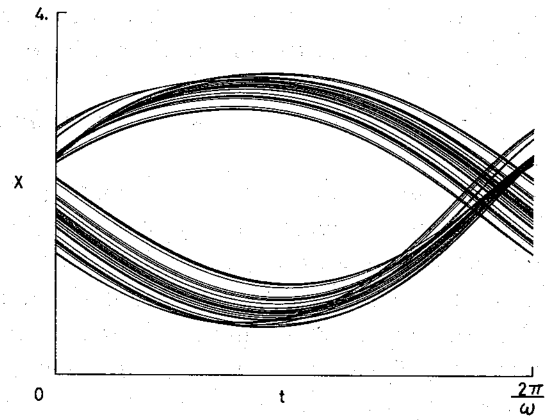


Fig. 8. The long time development of $x$ of one orbit where the right end of the orbit continues to the left end. The folding process is recognized on the lower band and the band is pressed on the beginning on the upper part, then it is enlarged during the last stage.

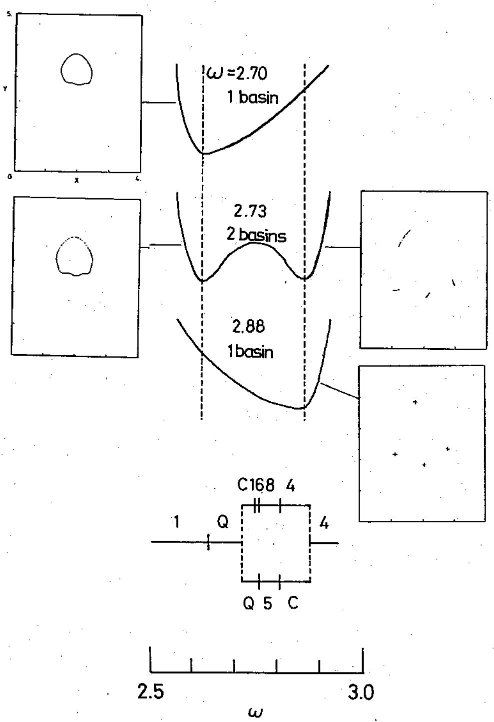


Fig. 9. The schematical illustration of the bifurcation and the unification phenomena of the basins. The left basin and the right basin correspond to the torus to chaos scenario and the Feigenbaum scenario, respectively. Poincaré mappings correspond to the basins.

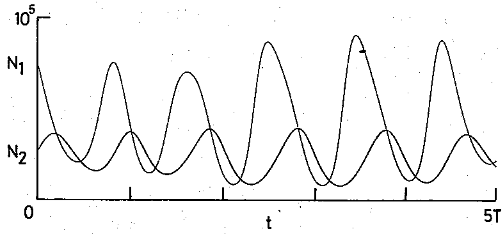


Fig. 10. Time evolutions of prey's population $N_1(t)$ and predator's population $N_2(t)$ for the chaotic state where parameters are taken as $a=\alpha_2=3.0$, $(\beta_1/2)=\beta_2=1.5\times10^{-2}$, $\gamma_1=0.48\times10^{-4}$, $b=0.17$ and $\omega=3.81$. In this parameter region there are two chaotic basins and the basins of the torus to chaos scenario is chosen. Obviously the number of the population is a natural number, however, we consider it as a positive real number in this paper.

ratio 4.669⋯.

In this section and the preceding section, we have investigated characters of motions in the frequency region $2.5\leqq\omega\leqq4.0$ where both the course $(2.5\to4.0)$ and $(4.0\to2.5)$ are considered. The scenario leading to chaos depends on the course and four bistable regions are observed as shown in Fig. 2. For example, there are two basins in the region $2.73\lesssim\omega\lesssim2.87$. A bifurcation and a unification phenomena of the basins are schematically illustrated in Fig. 9.

For ecologists, time evolutions of prey's population $N_1(t)=\{x(t)\}^2$ and predator's population $N_2(t)=y(t)$ for a chaotic state are shown in Fig. 10. The behaviors are similar to those of the mountain cat-hare community.[19]

## § 5. Discussion and some remarks

We have studied scenarios leading to chaos in the forced Lotka-Volterra model. Feigenbaum scenarios and the torus to chaos with frequency locking scenario are found and their scaling properties and hysteresis are investigated. From a biological point of view our results merely show that the forced predator-prey model has many different kinds of motions which include chaos. Real two-species ecosystem are very complicated. Therefore, the detail structures of the motions of our model have no important meaning in the sense of biology.

It is interesting that our model has some multi-basins for some ranges of parameters. In general, the existense of many basins brought us a rich structure in a system which obeys simple deterministic laws (a set of equations). One of the basins is chosen accidentally by its initial condition. This situation gives a *metaphor* that rich structures of nature are produced by *necessity* (simple deterministic laws) and *chance* (accidental chosen).

## Acknowledgements

The authors wish to thank Dr. H. Fujisaka for valuable discussions and comments. This study was partially financed by the Scientific Research Fund of the Ministry of Education, Science and Culture.

## References

1) H. Fujita and S. Utida, Ecology **34** (1953), 488.
S. Utida, Cold Spring Harb, Symp. Quant. Biol. **22** (1957), 139.
2) R. M. May, Science **186** (1974), 645; Nature **261** (1976), 459.
3) A. J. Nicholson, Cold Spring Harb. Symp. Quant. Biol. **22** (1957), 153.
4) S. Smale, J. Math. Biol. **3** (1976), 5.
5) A. Arneodo, P. Coullet and C. Tresser, Phys. Lett. **79A** (1980), 259.
6) M. J. Feigenbaum, Phys. Lett. **74A** (1979), 375; J. Stat. Phys. **19** (1978), 25.
7) A. Libchaber and J. Maurer, in *Nonlinear Phenomena at Phase Transitions and Instabilities,* ed. T. Riste (Plenum, N. Y. and London, 1981).
J. P. Gollub and S. V. Benson, J. Fluid Mech. **100** (1980), 449.
8) D. Rand, S. Ostlund, J. Sethna and E. Siggia, Phys. Rev. Lett. **49** (1982), 132.
9) S. J. Shenker, Physica **5D** (1982), 405.
10) K. Kaneko, Prog. Theor. Phys. **68** (1982), 669.
11) K. Kaneko, Prog. Theor. Phys. **69** (1983), 403.
12) L. Glass and R. Perez, Phys. Rev. Lett. **48** (1982), 1772.
R. Perez and L. Glass, Phys. Lett. **90A** (1982), 441.
13) M. Sano and Y. Sawada, Phys. Lett. **97A** (1983), 73.
14) See, e.g., N. S. Gole, S. C. Maitra and E. W. Montroll, Rev. Mod. Phys. **43** (1971), 231.
15) See, e.g., G. Nicolis and I. Prigogine, *Self-Organization in Nonequilibrium Systems* (John Wiley & Sons, N. Y., 1977).
16) R. M. May, Science **177** (1972), 900.
17) M. L. Rosenzweig, Science **171** (1971), 385 and references cited therein.
18) G. F. Gause, *The Struggle for Existence* (Williams & Wilkins, Baltimore, 1934).
19) R. M. May, *Stability and Complexity in Model Ecosystems* (Princeton U. P., 1974).
20) G. E. Hutchinson, Ann. N. Y. Acad. Sci. **50** (1948), 221.
21) H. Fujisaka, H. Kamifukumoto and M. Inoue, Prog. Theor. Phys. **69** (1983), 333.